British Journal of Pharmacology (2005) 144, 528–537
www.nature.com/bjp

Malonate induces cell death *via* mitochondrial potential collapse and delayed swelling through an ROS-dependent pathway

[1]Francisco J. Fernandez-Gomez, [1]Maria F. Galindo, [1]Maria Gómez-Lázaro, [2]Victor J. Yuste, [2]Joan X. Comella, [3]Norberto Aguirre & *,[1,4]Joaquín Jordán

[1]Departamento de Ciencias Médicas, Facultad de Medicina, Universidad de Castilla-La Mancha, Albacete, Spain; [2]Grup de Neurobiologia Molecular, Departmento de Ciencies Mediques Basiques, Universitat de Lleida, Spain; [3]Departamento de Farmacología, Facultad de Medicina, Universidad de Navarra, Pamplona, Spain and [4]Centro Regional de Investigaciones Biomédicas, Albacete, Spain

1 Herein we study the effects of the mitochondrial complex II inhibitor malonate on its primary target, the mitochondrion.

2 Malonate induces mitochondrial potential collapse, mitochondrial swelling, cytochrome *c* (Cyt *c*) release and depletes glutathione (GSH) and nicotinamide adenine dinucleotide coenzyme (NAD(P)H) stores in brain-isolated mitochondria.

3 Although, mitochondrial potential collapse was almost immediate after malonate addition, mitochondrial swelling was not evident before 15 min of drug presence. This latter effect was blocked by cyclosporin A (CSA), Ruthenium Red (RR), magnesium, catalase, GSH and vitamin E.

4 Malonate added to SH-SY5Y cell cultures produced a marked loss of cell viability together with the release of Cyt *c* and depletion of GSH and NAD(P)H concentrations. All these effects were not apparent in SH-SY5Y cells overexpressing Bcl-xL.

5 When GSH concentrations were lowered with buthionine sulphoximine, cytoprotection afforded by Bcl-xL overexpression was not evident anymore.

6 Taken together, all these data suggest that malonate causes a rapid mitochondrial potential collapse and reactive oxygen species production that overwhelms mitochondrial antioxidant capacity and leads to mitochondrial swelling. Further permeability transition pore opening and the subsequent release of proapoptotic factors such as Cyt *c* could therefore be, at least in part, responsible for malonate-induced toxicity.

British Journal of Pharmacology (2005) **144,** 528–537. doi:10.1038/sj.bjp.0706069
Published online 17 January 2005

Keywords: Bcl-xL; cytochrome *c*; mitochondria; malonate; neurodegeneration; ROS; glutathione; mitochondrial permeability transition; cytotoxicity

Abbreviations: A_{540}, absorbance at 540 nm; BSO, buthionine sulfoximine; COX-IV, cytochrome *c* oxidase subunit IV; CsA, cyclosporin A; Cyt *c*, cytochrome *c*; DMEM, Dulbecco's modified Eagle's medium; GSH, glutathione; LDH, lactate dehydrogenase; $\Delta\Psi_m$, mitochondrial potential; mBCl, monochlorobimane; MPTP, 1-methyl-4-phenyl-1,2,3,6-tetrahydropyride; NAD(P)H, nicotinamide adenine dinucleotide coenzyme ($NADH/NAD^+$) and its derivatives ($NADPH/NADP^+$); 3-NP, 3-nitorpropionic acid; 6-OHDA, 6-hydroxydopamine; PBS, phosphate buffered saline; PTP, permeability transition pore; ROS, reactive oxygen species; RR, ruthenium red; TCA, trichloroacetic acid; TMRE, tetramethylrhodamine ethyl ester

Introduction

Mitochondria are involved in a number of important cellular functions, including essential pathways of intermediate metabolism, amino-acid biosynthesis, fatty acid oxidation and steroid metabolism. Of key importance is the role of mitochondria in oxidative phosphorylation and apoptosis. Thus, mitochondria are considered the headquarters in apoptosis pathways (for a review, see Susin *et al*., 1998; Kroemer & Reed, 2000; Jordan *et al*., 2003). Many apoptotic stimuli cause either functional or morphological mitochondrial alterations such as collapse of the transmembranal potential or swelling. Hallmarks of these mitochondrial alterations are increased free radical production and release of cytochrome *c* (Cyt *c*) from mitochondria to the cytosol through the permeability transition pore (PTP) (Kroemer & Reed, 2000; Vila & Przedborski, 2003). The Bcl-2 family of proteins, which is implicated in the regulation of apoptosis by modulating PTP aperture, comprises members that have either antiapoptotic (such as Bcl-2 and Bcl-xL) or proapoptotic (such as Bax and Bak) effects (Brenner *et al*., 2000; Gross, 2001). In this sense, Bcl-2 or Bcl-xL overexpression has been shown to confer protection to cells exposed to apoptotic stimuli including staurosporine (Yuste *et al*., 2002), 6-hydroxydopamine (6-OHDA) (Galindo *et al*., 2004), 1-methyl-4-phenyl-1,2,3,6-tetrahydropyride (MPTP) (Yang *et al*., 1998) or 3-nitorpropionic acid (3-NP) (Bogdanov *et al*., 1999).

*Author for correspondence at: Facultad de Medicina, Centro Regional de Investigaciones Biomédicas, Universidad de Castilla-La Mancha, Avda. Almansa, s/n, 02006 Albacete, Spain;
E-mail: joaquin.jordan@uclm.es
Published online 17 January 2005

There is substantial evidence indicating that oxidative stress plays a role in the progression of a constellation of neurological disorders. Mitochondria have been proposed to be the main source of reactive oxygen species (ROS) in neuronal cells. Cells contain antioxidant systems to block ROS overproduction, including glutathione (GSH) and nicotinamide adenine dinucleotide coenzyme ($NADH/NAD^+$) and its derivatives ($NADPH/NADP^+$) (NAD(P)H), which play a crucial role as part of the primary cellular defence against oxidative stress. It has been shown that GSH levels in the cerebrospinal fluid decline during aging (Cudkowicz *et al*., 1999). The involvement of GSH in the control of cell death in neurodegenerative diseases is striking and it has been suggested that GSH depletion might be an upstream biochemical event in neurodegeneration (Dexter *et al*., 1989a, b). We and others have also observed a GSH depletion after different apoptotic stimuli including 6-OHDA (Galindo *et al*., 2004), veratridine (Jordan *et al*., 2002), MPTP (Selley, 1998) or malonate (Ehrhart & Zeevalk, 2003).

On the other hand, it is clear that impairment of mitochondrial energy metabolism is the key pathogenic factor in a number of neurodegenerative disorders (see review by Schon & Manfredi, 2003). Accordingly, toxins that affect mitochondria are being used as pharmacological tools to mimic several of these diseases. Among others, 3-NP, MPTP, rotenone and malonate are well-established mitochondrial complex inhibitors frequently used to investigate the key cellular pathways that provoke neurodegeneration in Parkinson's or Huntington's diseases (Browne & Beal, 2002).

Malonate has been shown to cause dose-dependent neurotoxicity both '*in vivo*' and '*in vitro*' by inhibition of succinate dehydrogenase and depletion of striatal ATP (Beal *et al*., 1993; Greene & Greenamyre, 1995; Stokes *et al*., 2001, Van Westerlaak *et al*., 2001) resulting in neuronal depolarization and secondary excitotoxicity (Henshaw *et al*., 1994; Greene & Greenamyre, 1996). In a recent study by Schulz *et al*. (1998), it was suggested that malonate toxicity involves neurons dying not only by secondary excitotoxicity but also by delayed caspase activation and apoptosis (Schulz *et al*., 1998). Thus, the exact mechanism by which malonate induces toxicity remains unclear.

The aim of this study was to analyse the role played by mitochondria in the mechanisms underlying malonate-induced cell death. We used isolated mitochondrial preparations to study the effect of malonate on this organelle. We present evidence showing that malonate induces mitochondrial potential collapse and depletion of mitochondrial antioxidant defence which leads to mitochondrial swelling and release of proapoptotic proteins including Cyt *c*. The role of the antiapoptotic protein Bcl-xL in these processes is also addressed.

Methods

Mitochondrial isolation

Mitochondria were isolated from the brains of adult Sprague–Dawley rats. All the procedures followed in the present work were in compliance with the European Community Council Directive of 24 November 1986 (86/609/EEC) and were approved by the Ethical Committee of the University of Castilla-La Mancha. To exclude that the observed effects were due to contaminating synaptosomes, we isolated brain mitochondria using a Percoll gradient as previously described (Sims, 1990). Rats were killed by decapitation, forebrains were rapidly removed, chopped and homogenized in ice-cold isolation buffer (225 mM mannitol, 25 mM sucrose, 10 mM Hepes, 1 mM K_2EDTA, pH 7.4 at 4°C). The homogenate was centrifuged at $1330 \times g$ for 3 min, and the pellet obtained was resuspended and recentrifuged at $1330 \times g$ for 3 min. The pooled supernatants were centrifuged at $21{,}300 \times g$ for 10 min. The pellet was resuspended in 15% Percoll and layered on preformed gradients (40 and 23%). The Percoll gradients were then centrifuged at $31{,}700 \times g$ for 10 min. The mitochondrial fraction located at the interface of the lower two layers was removed, diluted with isolation buffer and centrifuged at $16{,}700 \times g$ for 10 min. The mitocondrial pellet was resuspended in solution III (215 mM mannitol, 71 mM sucrose, 10 mM succinate and 10 mM HEPES, pH 7.4) and kept on ice for analysis.

Permeability transition pore activity

Permeability transition pore opening was assayed spectrophotometrically as previously described (Kristal *et al*., 2000). Specifically, mitochondria were suspended to reach a protein concentration of 1 mg ml^{-1} in 200 μl of solution containing 125 mM KCl, 20 mM Hepes, 2 mM KH_2PO_4, I μM EGTA, 1 mM $MgCl_2$, 5 mM malate and 5 mM glutamate with the pH adjusted to 7.08 with KOH. Changes in absorbance at 540 nm (A_{540}), indicating mitochondrial swelling due to PTP opening, were determined, after addition of different compounds, using a microplate reader (BioRad, Hercules, CA, U.S.A.). Initial A_{540} values were $\cong 0.8$, and minor differences in the loading of the wells were compensated by representing the data as the fraction of the initial absorbance determination remaining at a given time. Mitochondrial protein concentrations were quantified spectrophotometrically (Micro BCA Protein Reagent Kit), with bovine serum albumin used as standard.

Assay for NAD(P)H levels

Levels of NAD(P)H were determined using autofluorescence as previously described (Rover Jr *et al*., 1998). The chemical stability of nicotinamide adenine dinucleotide coenzyme ($NADH/NAD^+$) and its derivatives ($NADPH/NADP^+$) were investigated by using changes in the UV-visible absorption spectra of these compounds. We therefore refer to NAD(P)H, indicating the signal derived from either NADH or NADPH, or both. NAD(P)H fluorescence in intact mitochondria (1 mg ml^{-1} at 25°C) was measured fluorimetrically using excitation and emission wavelengths set at 340 nm (slit 3 nm) and 460 nm (slit 5 nm), respectively, in a Perkin–Elmer LS50B luminescence-spectrophotometer using a quartz cell with a 1 cm optical path as previously described (Rover Jr *et al*., 1998). On the day of the experiment, culture medium was removed, cells were washed three times with 1 ml of ice-cold phosphate-buffered saline (PBS), scraped into 500 μl 0.2% Triton X-100, centrifuged ($800 \times g$, 4°C, 5 min). Fluorescence was determined in 300 μl of the cell extract.

Measurement of GSH

Levels of GSH were determined by using monochlorobimane (mBCl) fluorescence. GSH is specifically conjugated with mBCl to form a fluorescent bimane-GSH adduct, in a reaction catalysed by glutathione *S*-transferases (Shrieve *et al*., 1988). The concentration of the bimane-GSH adduct increases during the initial 10–12 min period of this reaction with first-order kinetics, before levelling off (Young *et al*., 1994). Fluorescence levels at 15 min were used as an indication of intracellular GSH content, as it has been described previously (Shrieve *et al*., 1988). Culture medium was removed and cells were washed three times with 1 ml PBS (37°C) and incubated for 30 min at 37°C in 1 ml fresh PBS containing 80 μM mBCl. After incubation, cells were washed twice with ice-cold PBS and scraped in PBS, centrifuged and 300 μl of the extract was used for GSH determination. Fluorescence was measured at an excitation wavelength of 340 nm and emission wavelength of 460 nm. Protein content was determined by the bicinchoninic acid method.

Measurement of cell viability

SH-SY5Y cultures were grown in Dulbecco's modified Eagle's medium (DMEM) supplemented with 2 mM L-glutamine, penicillin (20 U ml^{-1}), streptomycin (5 μg ml^{-1}), and 15% (vol vol^{-1}) heat-inactivated fetal calf serum (GIBCO, Gaithersburg, MD, U.S.A.) as reported previously by Galindo *et al*. (2004). Cells were grown in a humidified cell incubator at 37°C under a 5% CO_2 atmosphere. For viability experiments, cells were plated at a density of 4×10^4 cells cm^{-2} and allowed to attach overnight. Cell viability after malonate additions was assessed by measurement of lactate dehydrogenase activity according to the protocol provided by the manufacturer (Promega). Briefly, the reaction mixture was added to conditioned media and removed from 24-well plate after centrifugation at $250 \times g$ for 10 min. Absorbance of samples at 490 nm was measured in a microplate reader (BioRad, Hercules, CA, U.S.A.) after 30 min of incubation at room temperature.

Cyt c *determinations*

Immunoblot analysis was performed on extramitochondrial extracts and cytosolic proteins. Briefly, isolated mitochondrial suspensions were treated with resuspension (control), malonate 1 and 10 mM) for 30 min and then centrifuged at 15,000 r.p.m. for 15 min. The supernatants, extramitochondrial fractions, were precipitated by trichloroacetic acid (TCA) (10%, 4°C overnight) and centrifuged ($15{,}000 \times g$; 15 min). Pellets were resuspended in 40 μl of loading buffer and boiled for 15 min. For culture experiments, cytosolic extracts from control and malonate-treated cultures were obtained as previously described (Maestre *et al*., 2003). Cells were washed once with PBS and collected by centrifugation ($2000 \times g$; 5 min). The cell pellet was resuspended in 200 μl of extraction buffer containing (mM): sucrose 250, Tris–HCl 50, EGTA 1, EDTA 1, DTT 1, PMSF 0.1, pH 7.4. Cells were homogenized in a Teflon-glass homogenizer (five strokes) and, after 15 min on ice, the suspension was centrifuged ($15{,}000 \times g$; 15 min). Supernatants, that is, cytosolic fractions, were removed and stored at −80°C until analysed by gel electrophoresis. TCA-samples or 15 μg of cytosolic proteins from control and treated conditions were loaded onto the same 15% SDS–polyacrylamide gel, separated and transferred to a PVDF membrane, that was incubated with anti-Cyt *c* (1 : 1000 dilution of rabbit polyclonal IgG, Santa Cruz Biotechnology Inc.). The signal was detected using an enhanced chemiluminescence detection kit (Amersham ECL RPN 2106 Kit). Analysis of cytosolic Cyt *c* from SH-SY5Y-Neo *versus* Bcl-xL overexpressing cells were performed on the same gel and lot for comparative purposes. cytochrome *c* oxidase subunit IV (COX-IV) protein levels were used as mitochondrial protein loading controls by using with antiCOX-IV (BD Biosciences).

Analysis of DNA fragmentation

The nuclear morphology of cells was studied by using the cell-permeable DNA dye Hoechst 33342. SH-SY5Y cells were cultured on poly-D-lysine-coated glass coverslips. Cells treated with malonate (100 mM, 24 h) were washed twice with PBS, stained with 5 μg ml^{-1} Hoechst 33342 for 5 min, and rinsed once with PBS. Cells were observed under an UV illumination microscope (excitation/emission 350/460 nm). Cells with homogeneously stained nuclei were considered to be viable, whereas the presence of chromatin condensation and/or fragmentation was indicative of apoptosis. Living and apoptotical cells were counted on adjacent fields of each coverslips totalling ~300–450 cells. The percentage of apoptotical cells was determined on three or four coverslips for each condition and normalized to parallel controls. Each independent coverslip was treated as a single observation, and at least three coverslips were used in each experiment. The average relative percent apoptotical from at least three separate cultures was determined.

Statistical analysis

Statistically significant differences between groups were determined by ANOVA followed by a Newman–Keuls *post hoc* analysis. The level of statistical significance was set at $P < 0.05$.

Materials

Most chemicals, including malonic acid, cyclosporin A (CsA), vitamin E, catalase, trichloroacetic acid and ruthenium red (RR) were obtained from Sigma (St Louis, MO, U.S.A.). Monochlorobimane, tetramethylrhodamine ethyl ester (TMRE) and Hoechst 33342 were purchased from Molecular Probes, Inc., (Eugene, OR, U.S.A.). The Micro BCA Protein Reagent Kit and Lactate dehydrogenase activity kit came from Pierce (Rockford, IL, U.S.A.) and from Promega (Madison, WI, U.S.A.) respectively. Monoclonal anti-Cyt *c* was purchased from R&D system (Minneapolis, MN, U.S.A.) and anti-COX-IV from BD Biosciences (Heidelberg, Germany).

Results

Malonate induces a delayed mitochondrial swelling and Cyt c *release*

Mitochondria are key players in triggering apoptosis signalling pathways that lead to cell death (Susin *et al*., 1998). In the first set of experiments, we investigated whether malonate would induce mitochondrial swelling in isolated mitochondria by monitoring 540 nm absorbance (A_{540}) decrease, and its effect was compared to that produced by a control stimuli, $CaCl_2$. As shown in Figure 1 (top panel), malonate induced mitochondrial swelling. The mitochondria suspension did not respond to malonate as quickly as it did after $CaCl_2$ additions. While mitochondria started to swell right after Ca^{2+} addition, malonate did not significantly modify mitochondrial suspension absorbance at times earlier than 20 min. By 10 min, mitochondrial suspension absorbance dropped around 5% of control values in malonate-treated mitochondria ($P>0.05$, $n=6$), while Ca^{2+}-induced decrease was around 20% at this time point ($P<0.01$, $n=6$) (Figure 1a). However, once malonate initiated mitochondrial swelling, mitochondrial suspension absorbance started to drop resulting in similar values to those achieved after Ca^{2+} additions at the end of the experiments (Figure 1b). Consistent with the well-established consequence of mitochondrial swelling, release of Cyt *c* was evident by 30 min after malonate addition (1 and 10 mM) (Figure 1c).

Next, we were interested in gaining insight into the mechanisms underlying malonate-induced mitochondrial swelling. To address this question, we performed a series of experiments using malonate (1 mM) in combination with drugs known to act through different mechanisms of action. The presence of CsA (10 μM) blocked malonate-induced changes in absorbance, suggesting the involvement of the PTP (Figure 2). As PTP opening is regulated by the external inhibitory Mg^{2+}-binding site (Bernardi *et al*., 1993), we added Mg^{2+} at a final concentration of 2 mM. As expected, Mg^{2+} also abolished malonate-induced swelling, confirming the role of PTP. As shown in Figure 2, blockade of Ca^{2+} influx, in the presence of the mitochondrial Ca^{2+} uptake blocker RR, also inhibited malonate-induced mitochondrial swelling. Finally, the role of ROS in malonate-induced mitochondrial swelling was assessed by using the broad lipophylic antioxidant vitamin E, the scavenger enzyme catalase (10 U mL^{-1}) or GSH (2.5 mM). Pretreatment with these antioxidant agents for 1 h caused a

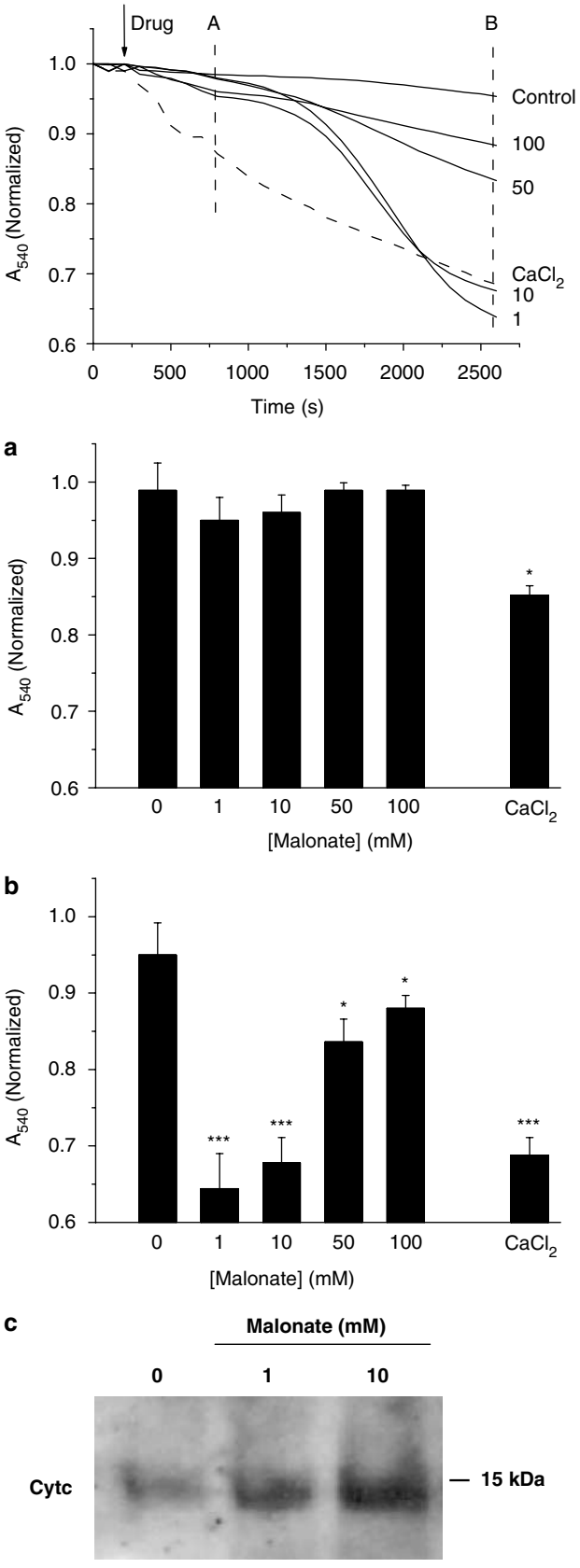

Figure 1 Malonate induces a delayed mitochondrial swelling. Mitochondrial swelling was followed by measuring changes in A_{540} in mitochondria suspensions. Malonate mediates a loss in absorbance in isolated mitochondria suspension. Different amounts of malonate, in a final volume of 25 μl, were added at 5 min as noted by the arrow. Final malonate concentrations are expressed at the end of traces. Trace control represents no added drug, and 25 μl of buffer were added to control for dilution effects. Dashed line represent $CaCl_2$ (75 μM) addition. Data represent mean values obtained from one experiment performed in triplicate. Histograms represent means$\pm$s.e.m. of changes in absorbance at 600 (a) and 2400 s (b) after drug additions from five experiment performed by triplicate. $^*P<0.05$; $^{***}P<0.001$. (c) Malonate induces Cyt *c* release. Mitochondria were incubated during 30 min with resuspension (control) or malonate (1,10 mM) and then centrifuged for 15 min at 15,000 r.p.m. at 4°C. Protein precipitated overnight with 10% TCA is shown. Pellets were subjected to polyacrylamide gel electrophoresis and immunoblot analysis using an antibody that recognizes Cyt *c*.

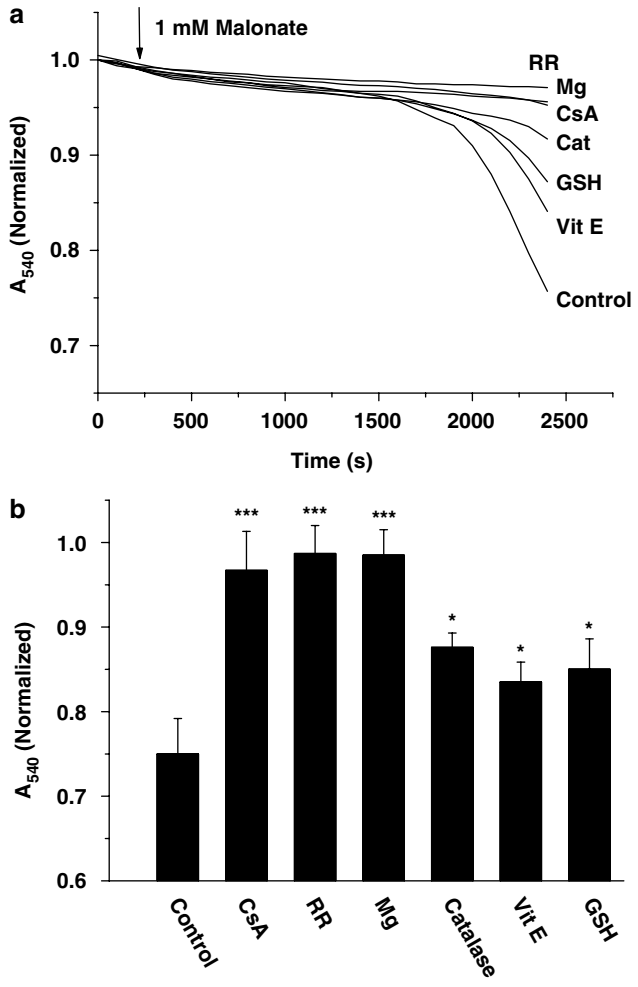

Figure 2 Role of calcium and ROS in malonate-induced mitochondrial swelling. Malonate addition (1 mM/500 μg protein; arrow) induces mitochondrial swelling in isolated mitochondria in an PTP-sensitive manner. Mitochondrial suspensions were incubated during 15 min with Cyclosporin A (CsA, 10 μM), Magnesium (Mg, 2 mM), Ruthenium Red (RR, 5 μM) or 1 h with Vitamin E (Vit E, 50 μM), Catalase (Cat, 10 U mL^{-1}) and Glutathione (GSH, 2.5 mM) prior to addition of malonate. Control nontreated mitochondria are also shown. Lines represent mean values of one experiment performed in triplicate. Histogram panels represent mean values $\pm$ s.e.m. of normalised A_{540} at 2200 s from at least five different mitochondrial preparations. $^{*}P<0.05$; $^{***}P<0.001$ Students unpaired *t*-test.

slight but significant blockade of malonate-induced swelling (Figure 2).

Malonate induces mitochondrial potential collapse

In some apoptotic models, changes in mitochondrial potential ($\Delta\Psi_m$) take place. To address the plausible effect of malonate on $\Delta\Psi_m$, we monitored the release of TMRE, a cationic membrane-permeant fluorescent probe, from preloaded mitochondria. Under these conditions, total fluorescence of mitochondrial suspension will increase if the organelles depolarise. Mitochondria responded to malonate releasing TMRE in a concentration-dependent manner, indicating that malonate additions result in $\Delta\Psi_m$ collapse. As shown in Figure 3, the time required for malonate to induce $\Delta\Psi_m$ collapse was shorter than that required to induce mitochondrial swelling.

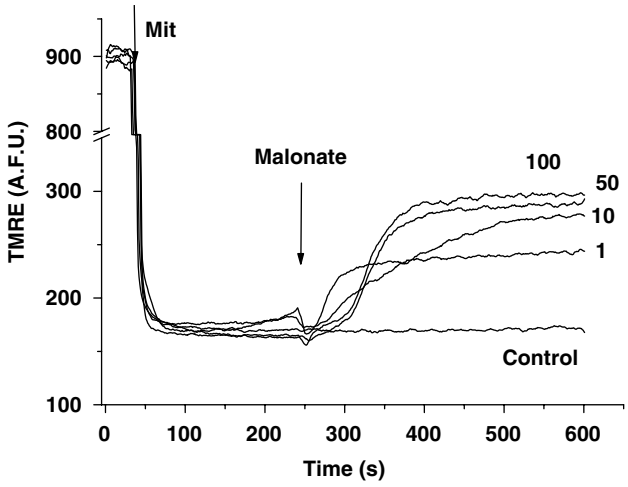

Figure 3 Malonate induces mitochondrial potential collapse. Mitochondrial membrane potential was measured by using TMRE. Addition of mitochondria (Mit, 500 protein μg) caused a decrease in fluorescence intensity due to TMRE uptake. Malonate (1–100 mM) was added at 240 s. Final malonate concentrations are expressed at the end of traces. Data are expressed as mean values obtained from one experiment performed in triplicate. Similar data were found in at least four different experiments.

Malonate disrupts mitochondrial redox state

GSH and NAD(P)H belong to the antioxidant systems used by cells to prevent ROS damage. In the next set of experiments, we analysed whether malonate could compromise these two ROS scavenger systems. To address this issue, we treated mitochondrial suspensions with different concentrations of malonate (1–100 mM) and 15 min later, GSH and NAD(P)H levels were determined. Our results show that malonate depletes these two antioxidant agents in a concentration-dependent manner (Figure 4), suggesting that it causes enough ROS to overwhelm mitochondrial antioxidant capacity.

Bcl-xL overexpression blocks malonate-induced cell death

Bcl-xL is an antiapototic protein located in the mitochondria that has been shown to block cell death under several paradigms, including those mediated by ROS (Vander Heiden *et al*., 1997). In the next set of experiments, we used the neuroblastoma cell line SH-SY5Y to investigate the role of this antiapoptotic protein in malonate-induced toxicity. Cell cultures were either stably transfected with DNA containing the open reading frame of Bcl-xL subcloned into pcDNA3 (SH-SY5Y/Bcl-xL) or with empty/pcDNA3 (SH-SY5Y/Neo) (Yuste *et al*., 2002). We used the lactate dehydrogenase (LDH) cell viability assay method to analyse the effects of malonate (0.1–100 mM) on SH-SY5Y cell viability. The lower concentrations of malonate tested, up to 10 mM, did not compromise cell viability, while higher concentrations (50–100 mM) resulted in gross morphological changes (data not shown). Staining of these cells with the DNA-binding dye, Hoechst 33342, showed chromatin condensation and fragmentation as compared to control cells (100 mM, about 40%, Figure 5b). The overexpression of Bcl-xL protein protected SH-SY5Y cells

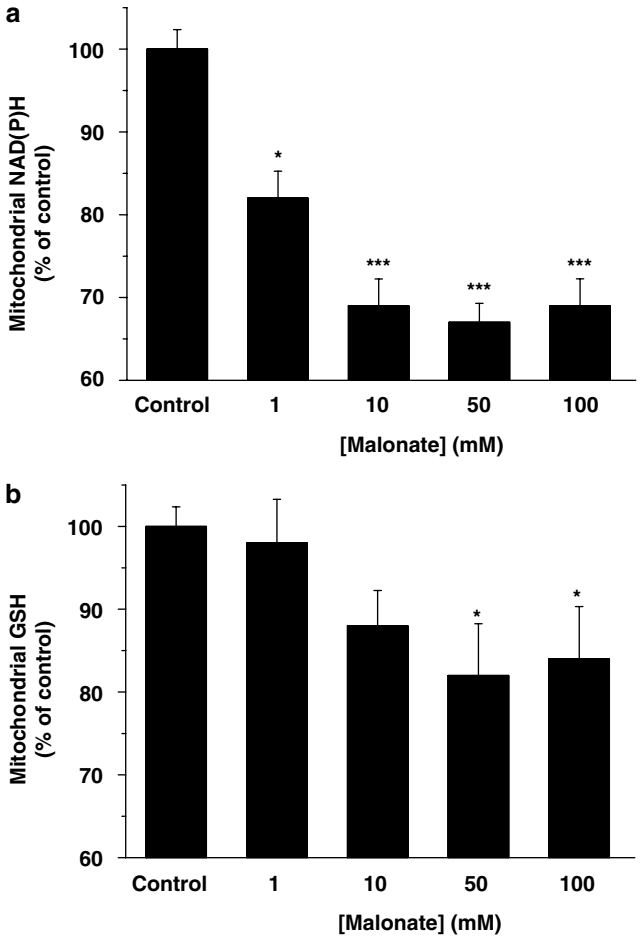

Figure 4 Malonate induces mitochondrial antioxidant stores depletion. Mitochondrial levels of NAD(P)H (a) or GSH (b) were determined after different malonate concentration additions 15 min after treatments. The values were expressed as a percentage of the autofluorescence (NAD(P)H) or mBCl fluorescence (GSH) from control conditions. Data represent means ± s.e.m. of at least 5 experiments performed in quadruplicate. (*$P<0.05$; ***$P< 0.001$).

against 100 mM malonate-induced toxicity (about 9%, Figure 5c).

It has been proposed that Bcl-xL might prevent the increase in mitochondrial membrane permeability which results in the release of mitochondrial apoptogenic factors such as Cyt *c* (Jordan *et al*., 2004). Consistent with the above data we found an increase in Cyt *c* levels into the cytoplasmic fraction obtained from SH-SY5Y/Neo cultures exposed to 50 mM

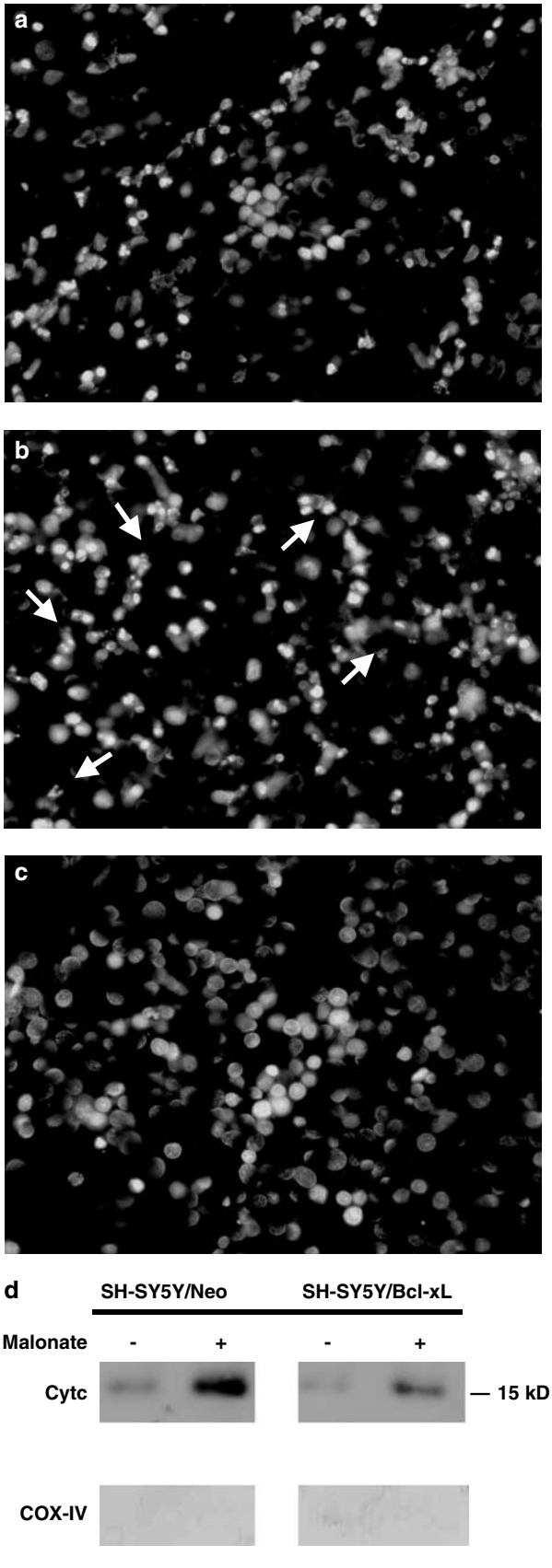

Figure 5 Effects of malonate on chromatin and Cyt *c* release in SH-SY5Y cultures. (a) Untreated SH-SY5Y/Neo cells were stained with the dye Hoechst 33342 as indicated in Methods. Normal nuclei without signs of chromatin fragmentation can be observed. (b, c) Cells exposed to malonate (100 mM) and stained with Hoechst 24 h later. Chromatin fragmentation is evident in SH-SY5Y/Neo cells cultures (b, arrows), but not in SH-SY5Y/Bcl-xL cells (c). (d) Malonate induces translocation of Cyt *c* that is blocked by Bcl-xL overexpression. Cytosolic extracts from SH-SY5Y/Neo and SH-SY5Y/Bcl-xL cells treated with 50 mM malonate for 12 h and assayed for Cyt *c* by Western blot technique. COX-IV protein levels were used as index of mitochondrial marker. The figure shows a representative experiment that was repeated three times with similar results.

malonate for 12 h. The overexpression of Bcl-xL blocked this release (Figure 5d).

In order to investigate whether cellular antioxidant systems were depleted in this model, NAD(P)H and GSH levels were evaluated. SH-SY5Y cell cultures were treated with different concentrations of malonate (0.1–100 mM), and the antioxidant levels were determined 24 h later. Consistent with the role of ROS in malonate-induced cell death, we found a large decrease in both antioxidant concentrations (Figure 6b and c). Moreover, Bcl-xL overexpression prevented cellular NAD(P)H and GSH from being oxidized (Figure 6b and c). To analyse whether Bcl-xL could be mediating cell protection by preventing antioxidant depletion, we pretreated SH-SY5Y/Bcl-xL cell cultures for 12 h with 100 μM buthionine sulphoximine (BSO) in order to decrease GSH levels to around 50% of the basal levels (Galindo *et al*., 2004). Under such experimental conditions, Bcl-xL-mediated cytoprotection was not evident anymore (Figure 6d).

Discussion

Consistent with the well-known inhibitory effect on mitochondrial complex II, the results reported here demonstrate that malonate induces cell death through a mechanism that involves a direct participation of the mitochondrion. Malonate induces a rapid depolarization of the mitochondrial electric potential and a delayed swelling of the organelle. Malonate increased the rate of ROS formation in mitochondria resulting in the depletion of ROS scavenger systems including GSH and NAD(P)H lelvels. On the other hand, the overexpression of the antiapoptotic mitochondrial located protein, Bcl-xL, blocked malonate-induced antioxidant systems depletion and cell death in SH-SY5Y cell cultures.

Malonate induces $\Delta\Psi_m$ collapse and mitochondrial swelling, pivotal events that have been described in several cellular apoptotic pathways (Fiskum, 2000; Gorman *et al*., 2000; Jordan *et al*., 2003). The kinetics of these effects seem to be different since the effect of malonate on $\Delta\Psi_m$ was almost immediate, while the drug was required to be present for at least 15 min before in order to start inducing mitochondrial swelling.

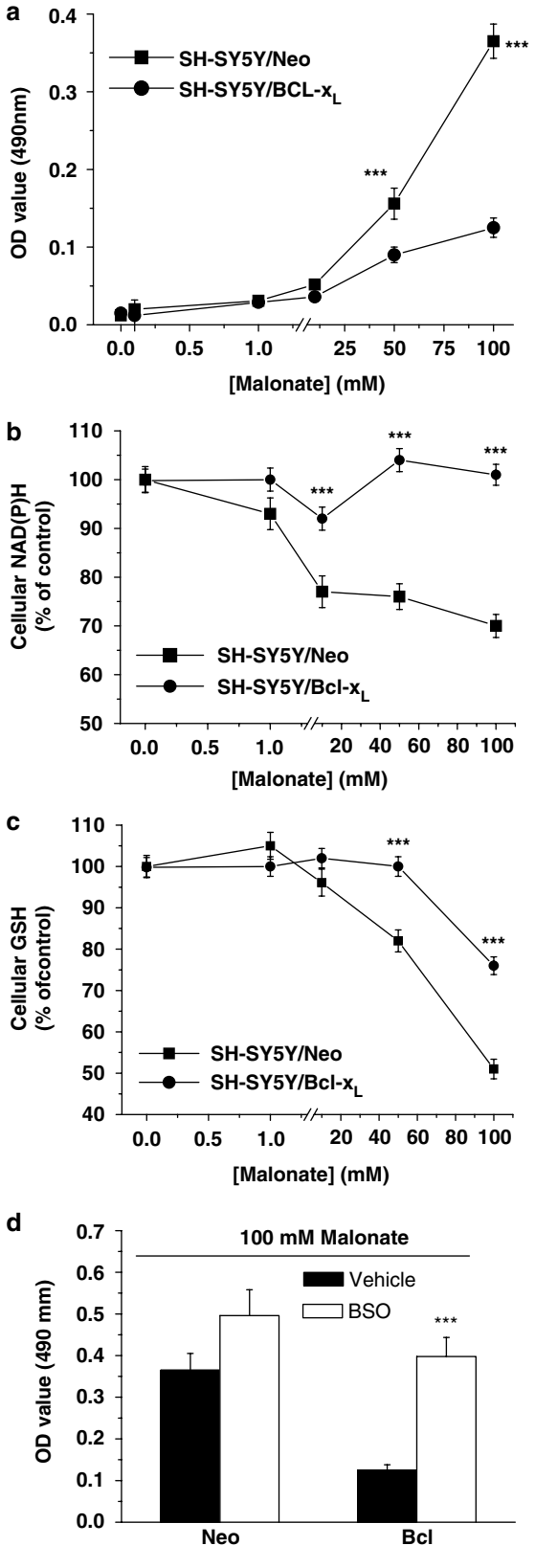

Figure 6 Bcl-xL-overexpression blocked malonate-induced cell death by preventing cellullar antioxidant stores depletion. (a) Malonate induced cell viability drop in SH-SY5Y cells cultures that was blocked by the overepression of Bcl-XL. Cell viability was assayed 24 h after malonate treatment. Culture media were collected and analysed for LDH release as an indicator of cell death. Data are presented as mean ± s.e.m. of percentage of untreated SH-SY5Y cells of four different experiments (***$P<0.01$). (b, c) Bcl-xL overexpression blocks malonate-mediated depletion of cellular antioxidant stores. Levels of NAD(P)H (b) and GSH (c) in SY-SY5Y cells cultures were determined 24 h after treatments. Values are expressed as a percentage of the autofluorescence (NAD(P)H) or mBCl fluorescence (GSH) from untreated conditions. Data represent means ± s.e.m. of at least five experiments performed in quadruplicate. (***$P<0.001$). (d) Effect of GSH depletion on SH-SY5Y cell survival. BSO (100 μM) were present 12 h before 100 mM malonate and maintained during the experiment. LDH release was measured 24 h later. Data represent mean ± s.e.m. of five different experiments. ***$P<0.001$ as compared with cells in the absence of BSO.

The precise mechanism by which malonate induced PTP formation remains difficult to understand. It is well established that either Ca^{2+} or ROS are able to induce PTP opening (Atlante *et al*., 2000). It is known that the inhibition of the respiratory chain alters electron transport and the proton motive force, which affects the synthesis of ATP and the transport of ions like Ca^{2+} (Crompton, 2000). Thus, it has been proposed that Ca^{2+} modulates PTP formation in conditions where intracellular [Ca^{2+}] is found to be high in a maintained manner (Galindo *et al*., 2003). Under such conditions, mitochondria are not able to increase mitochondrial [Ca^{2+}] indefinitely, and eventually release their Ca^{2+} by increasing the inner mitochondria membrane permeability through the PTP formation (Bernardi *et al*., 1998; Bernardi, 1999). On the other hand, ROS induce PTP formation by oxidation of thiol residues and, in some cases, by acting on the adenine nucleotide translocator eliminating its specificity or enhancing its sensibility to Ca^{2+} (Costantini *et al*., 2000). This latter hypothesis takes relevance in our conditions where ROS, GSH and NAD(P)H measurements show that malonate required minutes to disrupt mitochondrial redox status, likewise the time necessary for mitochondria to swell. According to our data, it appears that ROS may decline mitochondrial Ca^{2+} buffer capacity, making Ca^{2+} the main factor responsible for malonate-induced mitochondrial swelling. Supporting this hypothesis our data show that the blockade of Ca^{2+} influx by the presence of the mitochondrial Ca^{2+} uptake blocker, RR or magnesium completely blocked this event, while the presence of the broad antioxidant scavenger, vitamin E, or the peroxide scavenger enzyme catalase only inhibited mitochondrial swelling partially. Thus, it is possible that malonate, by inducing $\Delta\Psi_m$ collapse and subsequent ROS production, could make mitochondria more sensitive to possible changes in cytoplasmic [Ca^{2+}]. This latter hypothesis would explain why different NMDA antagonists, such as MK-801, protect against malonate toxicity but do not block the generation of hydroxyl radicals (Ferger *et al*., 2003), showing that oxidative stress during energy impairment caused by malonate is independent of glutamate receptor overstimulation and occurs at time points that precede secondary excitotoxicity (Zeevalk *et al*., 1998; 2000).

We also found that malonate depletes both of the main antioxidant systems used by cells to block ROS overproduction, GSH and NAD(P)H. Altered GSH/GSSG ratios have been shown in different neurodegenerative diseases (Cecchi *et al*., 1999; Bharath *et al*., 2002) and might be an upstream biochemical event leading to neurodegeneration (Dexter *et al*., 1989a, b). It has been recently reported that caspase inhibition protects neurons from malonate-induced striatal injury in rats (Toulmond *et al*., 2004), suggesting a crucial role for apoptosis in the mechanisms leading to cell death. Our data support this contention as the overexpression of the antiapoptotic Bcl-xL protein prevented malonate-induced toxicity in SH-SY5Y cells. Furthermore, Bcl-xL overexpression also prevented Cyt *c* release and depletion of both cellular antioxidant agents, GSH and NAD(P)H, caused by malonate. Since GSH depletion occurs after different apoptotic stimuli including 6-OHDA (Galindo *et al*., 2004) or veratridine (Jordan *et al*., 2002), we went further to study the relationship between GSH, Bcl-xL and cell death induced by malonate. For this reason, we pretreated Bcl-xL-overexpressing cells for 12 h with the GSH synthesis inhibitor, L-BSO and found that GSH depletion completely abolishes Bcl-xL antiapoptotic capacity, which attest to the prominent role of GSH as a first line of defence against ROS-induced cell death. Not surprisingly, increased levels of both lipid peroxidation and DNA oxidation by-product 8-hydroxy-deoxyguanosine are consistently found in the brains of acute (ischemia) or chronic neurodegenerative disease patients (e.g. Dexter *et al*., 1989a, b; Alam *et al*., 1997; Cutler *et al*., 2004).

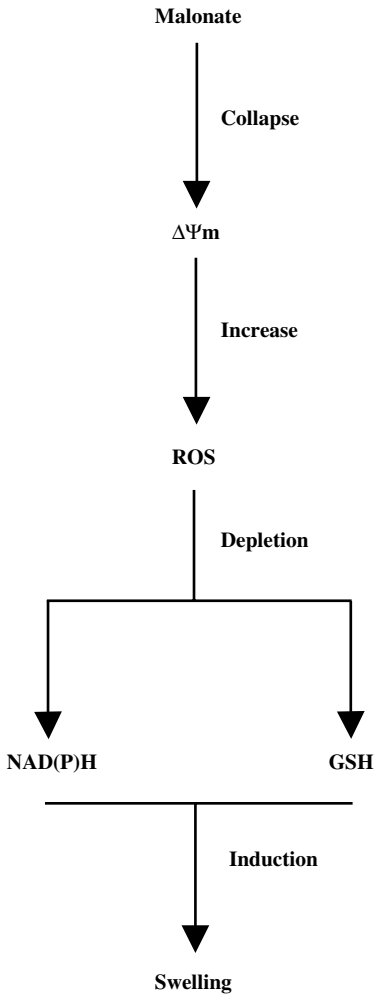

Figure 7 Schematic model summarising our findings. There is evidence that mitochondrial potential collapse and ROS production is increased and result in a depletion in mitochondrial antioxidant defence that results in mitochondrial swelling.

According to the data shown in this study, a plausible sequential model, regarding mitochondria, for malonate toxicity could be the following (Figure 7): malonate induces mitochondrial potential collapse and ROS production that result in the depletion of mitochondrial antioxidant defence yielding to mitochondrial swelling and release of proapoptotic proteins such as Cyt *c* responsible for the starting of the apoptotic machinery. This contention is consistent with two recent works showing that malonate toxicity is prevented by caspase-3 inhibitors (Toulmond *et al*., 2004) and also that the irreversible complex II inhibitor, 3-nitropropionic acid, causes mitochondrial collapse and oxidative stress in mice cortical astrocytes (Rosenstock *et al*., 2004).

We are grateful to the excellent technical work of Juana Rozalén. This work has been supported by SAF2002-04721 from CICYT and Almirall Prodesfarma to J.J. F.J. F-G, M. G-L and M.F.G. are fellows from JCCM.

References

ALAM, Z.I., JENNER, A., DANIEL, S.E., LEES, A.J., CAIRNS, N., MARSDEN, C.D., JENNER, P. & HALLIWELL, B. (1997). Oxidative DNA damage in the parkinsonian brain: an apparent selective increase in 8-hydroxyguanine levels in substantia nigra. *J. Neurochem.,* **69,** 1196–1203.

ATLANTE, A., CALISSANO, P., BOBBA, A., AZZARITI, A., MARRA, E. & PASSARELLA, S. (2000). Cytochrome *c* is released from mitochondria in a reactive oxygen species (ROS)-dependent fashion and can operate as a ROS scavenger and as a respiratory substrate in cerebellar neurons undergoing excitotoxic death. *J. Biol. Chem.,* **275,** 37159–37166.

BEAL, M.F., BROUILLET, E., JENKINS, B., HENSHAW, R., ROSEN, B. & HYMAN, B.T. (1993). Age-dependent striatal excitotoxic lesions produced by the endogenous mitochondrial inhibitor malonate. *J. Neurochem.,* **61,** 1147–1150.

BERNARDI, P. (1999). Mitochondrial transport of cations: channels, exchangers, and permeability transition. *Physiol. Rev.,* **79,** 1127–1155.

BERNARDI, P., COLONNA, R., COSTANTINI, P., ERIKSSON, O., FONTAINE, E., ICHAS, F., MASSARI, S., NICOLLI, A., PETRONILLI, V. & SCORRANO, L. (1998). The mitochondrial permeability transition. *Biofactors,* **8,** 273–281.

BERNARDI, P., VERONESE, P. & PETRONILLI, V. (1993). Modulation of the mitochondrial cyclosporin A-sensitive permeability transition pore. I. Evidence for two separate Mg^{2+} binding sites with opposing effects on the pore open probability. *J. Biol. Chem.,* **268,** 1005–1010.

BHARATH, S., HSU, M., KAUR, D., RAJAGOPALAN, S. & ANDERSEN, J.K. (2002). Glutathione, iron and Parkinson's disease. *Biochem. Pharmacol.,* **64,** 1037–1048.

BOGDANOV, M.B., FERRANTE, R.J., MUELLER, G., RAMOS, L.E., MARTINOU, J.C. & BEAL, M.F. (1999). Oxidative stress is attenuated in mice overexpressing BCL-2. *Neurosci. Lett.,* **262,** 33–36.

BRENNER, C., CADIOU, H., VIEIRA, H.L., ZAMZAMI, N., MARZO, I., XIE, Z., LEBER, B., ANDREWS, D., DUCLOHIER, H., REED, J.C. & KROEMER, G. (2000). Bcl-2 and Bax regulate the channel activity of the mitochondrial adenine nucleotide translocator. *Oncogene,* **19,** 329–336.

BROWNE, S.E. & BEAL, M.F. (2002). Toxin-induced mitochondrial dysfunction. *Int. Rev. Neurobiol.,* **53,** 243–279.

CECCHI, C., LATORRACA, S., SORBI, S., IANTOMASI, T., FAVILLI, F., VINCENZINI, M.T. & LIGURI, G. (1999). Glutathione level is altered in lymphoblasts from patients with familial Alzheimer's disease. *Neurosci. Lett.,* **275,** 152–154.

COSTANTINI, P., BELZACQ, A.S., VIEIRA, H.L., LAROCHETTE, N., DE PABLO, M.A., ZAMZAMI, N., SUSIN, S.A., BRENNER, C. & KROEMER, G. (2000). Oxidation of a critical thiol residue of the adenine nucleotide translocator enforces Bcl-2-independent permeability transition pore opening and apoptosis. *Oncogene,* **19,** 307–314.

CROMPTON, M. (2000). Mitochondrial intermembrane junctional complexes and their role in cell death. *J. Physiol.,* **529,** 11–21.

CUDKOWICZ, M.E., SEXTON, P.M., ELLIS, T., HAYDEN, D.L., GWILT, P.R., WHALEN, J. & BROWN JR, R.H. (1999). The pharmacokinetics and pharmaco-dynamics of Procysteine in amyotrophic lateral sclerosis. *Neurology,* **52,** 1492–1494.

CUTLER, R.G., KELLY, J., STORIE, K., PEDERSEN, W.A., TAMMARA, A., HATANPAA, K., TRONCOSO, J.C. & MATTSON, M.P. (2004). Involvement of oxidative stress-induced abnormalities in ceramide and cholesterol metabolism in brain aging and Alzheimer's disease. *Proc. Natl. Acad. Sci. U.S.A.,* **101,** 2070–2075.

DEXTER, D.T., CARTER, C.J., WELLS, F.R., JAVOY-AGID, F., AGID, Y., LEES, A., JENNER, P. & MARSDEN, C.D. (1989a). Basal lipid peroxidation in substantia nigra is increased in Parkinson's disease. *J. Neurochem.,* **52,** 381–389.

DEXTER, D.T., SIAN, J., ROSE, S., HINDMARSH, J.G., MANN, V.M., COOPER, J.M., WELLS, F.R., DANIEL, S.E., LEES, A.J. & SCHAPIRA, A.H. (1989b). Indices of oxidative stress and mitochondrial function in individuals with incidental Lewy body disease. *Ann. Neurol.,* **35,** 38–44.

EHRHART, J. & ZEEVALK, G.D. (2003). Cooperative interaction between ascorbate and glutathione during mitochondrial impairment in mesencephalic cultures. *J. Neurochem.,* **86,** 1487–1497.

FERGER, B., EBERHARDT, O., TEISMANN, P., DE GROOTE, C. & SCHULZ, J.B. (2003). Malonate-induced generation of reactive oxygen species in rat striatum depends on dopamine release but not on NMDA receptor activation. *J. Neurochem.,* **73,** 1329–1332.

FISKUM, G. (2000). Mitochondrial participation in ischemic and traumatic neural cell death. *J. Neurotrauma.,* **17,** 843–855.

GALINDO, M.F., JORDAN, J., GONZALEZ-GARCIA, C. & CEÑA, V. (2003). Reactive oxygen species induce swelling and cytochrome *c* release but not transmembrane depolarization in isolated rat brain mitochondria. *Br. J. Pharmacol.,* **139,** 797–804.

GALINDO, M.F., JORDAN, J., TORNERO, D., GONZÁLEZ-GARCÍA, C. & CEÑA, V. (2004). Bcl-x_L blocks mitochondrial multiple conductance channel activation and inhibits 6-OHDA-induced death in SH-SY5Y cells. *J. Neurochem.,* **89,** 124–133.

GORMAN, A.M., CECCATELLI, S. & ORRENIUS, S. (2000). Role of mitochondria in neuronal apoptosis. *Dev. Neurosci.,* **22,** 348–358.

GREENE, J.G. & GREENAMYRE, J.T. (1996). Manipulation of membrane potential modulates malonate-induced striatal excitotoxicity *in vivo*. *J. Neurochem.,* **66,** 637–643.

GREENE, J.G. & GREENAMYRE, J.T. (1995). Characterization of the excitotoxic potential of he reversible succinate dehydrogenase inhibitor malonate. *J. Neurochem.,* **64,** 430–436.

GROSS, A. (2001). BCL-2 proteins: regulators of the mitochondrial apoptotic program. *IUBMB Life,* **52,** 231–236.

HENSHAW, R., JENKINS, B.G., SCHULZ, J.B., FERRANTE, R.J., KOWALL, N.W., ROSEN, B.R. & BEAL, M.F. (1994). Malonate produces striatal lesions by indirect NMDA receptor activation. *Brain Res.,* **647,** 161–166.

JORDAN, J., CEÑA, V. & PREHN, J.H. (2003). Mitochondrial control of neuron death and its role in neurodegenerative disorders. *J. Physiol. Biochem.,* **59,** 129–141.

JORDAN, J., GALINDO, M.F., TORNERO, D., BENAVIDES, A., GONZALEZ, C., AGAPITO, M.T., GONZALEZ-GARCIA, C. & CEÑA, V. (2002). Superoxide anions mediate veratridine-induced cytochrome *c* release and caspase activity in bovine chromaffin cells. *Br. J. Pharmacol.,* **137,** 993–1000.

KRISTAL, B.S., STAATS, P.N. & SHESTOPALOV, A.I. (2000). Biochemical characterization of the mitochondrial permeability transition in isolated forebrain mitochondria. *Dev. Neurosci.,* **22,** 376–383.

KROEMER, G. & REED, J.C. (2000). Mitochondrial control of cell death. *Nat. Med.,* **6,** 513–519.

MAESTRE, I., JORDAN, J., CALVO, S., REIG, J.A., CENA, V., SORIA, B., PRENTKI, M. & ROCHE, E. (2003). Mitochondrial dysfunction is involved in apoptosis induced by serum withdrawal and fatty acids in the beta-cell line INS-1. *Endocrinology,* **144,** 335–345.

ROSENSTOCK, T.R., CARVALHO, A.C.P., JURKIEWICZ, A., FRUSSA-FILHO, R. & SMAILI, S.S. (2004). Mitochondrial calcium, oxidative stress and apoptosis in a neurodegenerative disease model induced by 3-nitropropionic acid. *J. Neurochem.,* **88,** 1220–1228.

ROVER JR, L., FERNANDES, J.C., DE OLIVEIRA NETO, G., KUBOTA, L.T., KATEKAWA, E. & SERRANO, S.H. (1998). Study of NADH stability using ultraviolet-visible spectrophotometric analysis and factorial design. *Anal. Biochem.,* **260,** 50–55.

SCHON, E.A. & MANFREDI, G. (2003). Neuronal degeneration and mitochondrial dysfunction. *J. Clin. Invest.,* **111,** 303–312.

SCHULZ, J.B., WELLER, M., MATTHEWS, R.T., HENEKA, M.T., GROSCURTH, P., MARTINOU, J.C., LOMMATZSCH, J., VON COELLN, R., WULLNER, U., LOSCHMANN, P.A., BEAL, M.F., DICHGANS, J. & KLOCKGETHER, T. (1998). Extended therapeutic window for caspase inhibition and synergy with MK-801 in the treatment of cerebral histotoxic hypoxia. *Cell Death Differ.,* **5,** 847–857.

SELLEY, M.L. (1998). E)-4-hydroxy-2-nonenal may be involved in the pathogenesis of Parkinson's disease. *Free Radic. Biol. Med.,* **25,** 169–174.

SHRIEVE, D.C., BUMP, E.A. & RICE, G.C. (1988). Heterogeneity of cellular glutathione among cells derived from a murine fibrosarcoma or a human renal cell carcinoma detected by flow cytometric analysis. *J. Biol. Chem.,* **263,** 14107–14114.

SIMS, N.R. (1990). Rapid isolation of metabolically active mitochondria from rat brain and subregions using Percoll density gradient centrifugation. *J. Neurochem.,* **55,** 698–707.

STOKES, A.H., BERNARD, L.P., NICKLAS, W.J. & ZEEVALK, GD. (2001). Attenuation of malonate toxicity in primary mesencephalic cultures using the GABA transport blocker, NO-711. *J. Neurosci. Res.,* **64,** 43–52.

SUSIN, S.A., ZAMZAMI, N. & KROEMER, G. (1998). Mitochondria as regulators of apoptosis: doubt no more. *Biochim. Biophys. Acta,* **1366,** 151–165.

TOULMOND, S., TANG, K., BUREAU, Y., ASHDOWN, H., DEGEN, S., O'DONNELL, R., TAM, J., HAN, Y., COLUCCI, J., GIROUX, A., ZHU, Y., BOUCHER, M., PIKOUNIS, B., XANTHOUDAKIS, S., ROY, S., RIGBY, M., ZAMBONI, R., ROBERTSON, G.S., NG, G.Y., NICHOLSON, D.W. & FLUCKIGER, J.P. (2004). Neuroprotective effects of M826, a reversible caspase-3 inhibitor, in the rat malonate model of Huntington's disease. *Br. J. Pharmacol.,* **141,** 689–697.

VANDER HEIDEN, M.G., CHANDEL, N.S., WILLIAMSON, E.K., SCHUMACKER, P.T. & THOMPSON, C.B. (1997). Bcl-xL regulates the membrane potential and volume homeostasis of mitochondria. *Cell,* **91,** 627–637.

VAN WESTERLAAK, M.G., JOOSTEN, E.A., GRIBNAU, A.A., COOLS, A.R. & BAR, P.R. (2001). Differential cortico-motoneuron vulnerability after chronic mitochondrial inhibition *in vitro* and the role of glutamate receptors. *Brain Res.,* **922,** 243–249.

VILA, M. & PRZEDBORSKI, S. (2003). Targeting programmed cell death in neurodegenerative diseases. *Nat. Rev. Neurosci.,* **4,** 365–375.

YANG, L., MATTHEWS, R.T., SCHULZ, J.B., KLOCKGETHER, T., LIAO, A.W., MARTINOU, J.C., PENNEY JR, J.B., HYMAN, B.T. & BEAL, M.F. (1998). 1-Methyl-4-phenyl-1,2,3,6-tetrahydropyride neurotoxicity is attenuated in mice overexpressing Bcl-2. *J. Neurosci.,* **18,** 8145–8152.

YOUNG, P.R., CONNORSWHITE, A.L. & DZIDO, G.A. (1994). Kinetic analysis of the intracellular conjugation of monochlorobimane by IC-21 murine macrophage glutathione-S-transferase. *Biochim. Biophys. Acta,* **1201,** 461–465.

YUSTE, V.J., SANCHEZ-LOPEZ, I., SOLE, C., ENCINAS, M., BAYASCAS, J.R., BOIX, J. & COMELLA, J.X. (2002). The prevention of the staurosporine-induced apoptosis by Bcl-X(L), but not by Bcl-2 or caspase inhibitors, allows the extensive differentiation of human neuroblastoma cells. *J. Neurochem.,* **80,** 126–139.

ZEEVALK, G.D., BERNARD, L.P. & NICKLAS, W.J. (2000). Oxidative stress during energy impairment in mesencephalic cultures is not a downstream consequence of a secondary excitotoxicity. *Neuroscience,* **96,** 309–316.

ZEEVALK, G.D., BERNARD, L.P., SINHA, C., EHRHART, J. & NICKLAS, W.J. (1998). Excitotoxicity and oxidative stress during inhibition of energy metabolism. *Dev. Neurosci.,* **20,** 444–453.

(Received September 14, 2004
Revised October 8, 2004
Accepted October 18, 2004)